Editors' Suggestion

Bridging between laboratory and rotating-frame master equations for open quantum systems

Gal Shavit,[1] Baruch Horovitz,[2] and Moshe Goldstein[1]

[1]*Raymond and Beverly Sackler School of Physics and Astronomy, Tel Aviv University, Tel Aviv 6997801, Israel*

[2]*Department of Physics, Ben-Gurion University of the Negev, Beer Sheva 84105, Israel*

(Received 30 July 2019; published 27 November 2019)

The problem of a driven quantum system coupled to a bath and coherently driven is usually treated using either of two approaches: employing the common secular approximation in the laboratory frame (as usually done in the context of atomic physics) or in the rotating frame (prevailing in, e.g., the treatment of solid-state qubits). These approaches are applicable in different parts of the parameter space and yield different results. We show how to bridge between these two approaches by working in the rotating frame without employing the secular approximation with respect to the driving amplitude. This allows us to uncover unusual behaviors in regimes which were previously inaccessible or inadequately treated. Exceptional features such as the qualitative different evolution of the coherence, population inversion at a lower driving amplitude, and unique structure in the resonance fluorescence spectrum of the system are found. We argue that this generalized approach is essential for analyzing hybrid systems, with components that come from distinctly different regimes which can now be treated simultaneously, giving specific examples from recent experiments on quantum dots coupled to optical cavities, and single-spin electron paramagnetic resonance.

DOI: 10.1103/PhysRevB.100.195436

I. INTRODUCTION

Complete isolation of any realistic quantum system from its environment is not typically possible. Open quantum systems, i.e., systems that have some non-negligible interactions with an external environment, or "bath," evolve over time in a nonunitary fashion, inevitably leading to processes of relaxation, losses, and phase decoherence [1]. As these dissipative effects can significantly alter the properties of such systems, the study of open quantum systems and their evolution over time has important consequences for a myriad of different quantum devices and applications, perhaps most importantly in the field of quantum computation and information processing [2].

The dynamics of an open quantum system is typically captured by performing a perturbative expansion in the bath coupling strength, followed by integrating out all the bath variables. This leads to a master equation for the system degrees of freedom, usually represented by the reduced system density matrix $\rho \equiv \mathrm{Tr}_B\{\rho_{SB}\}$, where ρ_{SB} is the total system and bath density matrix, and $\mathrm{Tr}_B\{\dots\}$ is a trace over the bath degrees of freedom. One of the most prevalent forms of such equations is the *Lindblad master equation* [3,4]

$$\frac{d}{dt}\rho = -\frac{i}{\hbar}[H_S, \rho] + \mathcal{D}\rho, \tag{1}$$

where H_S its Hamiltonian of the system, controlling the unitary part of the time evolution, and $\mathcal{D}$ is the dissipator superoperator, which is of the Lindblad form $\mathcal{D}\rho = \sum_j \gamma_j (L_j \rho L_j^\dagger - \frac{1}{2}\{\rho, L_j^\dagger L_j\})$, with L_j's being a set of "quantum jump" operators, and γ_j's the rates governing the dissipative dynamics. It should be noted that the Lindblad master equation is the most general form of a master equation with Markovian dynamics (i.e., without "memory" effects) which preserves the positive semidefiniteness and trace (thus, normalization of probabilities) of the density matrix [3,4]. To arrive at (1) starting from the microscopic description of the system's dynamics and its interaction with the bath, one must make the Born-Markov approximation [1,5], which essentially coarse grains the time evolution of the system density matrix such that timescales shorter than the bath correlation time cannot be properly resolved. Another simplification, crucial in obtaining the Lindbladian form, will be particularly relevant in this work: *the secular approximation*, requiring that the dissipative dynamics is sufficiently slow as compared to the system internal timescale.

The case where the open quantum system is driven out of equilibrium is of utmost importance in the physics and design of quantum devices. Such devices must be controlled and manipulated in various ways in order for them to be useful. Whether preparing a qubit in a specific desired initial state [6], reading information off it, writing and storing information onto it [7], probing its current quantum state [8], or manipulating it by an intricate sequence of well-designed pulses [9,10], driving of a quantum system is a hallmark of quantum control and a staple of quantum engineering.

However, the introduction of the driving Hamiltonian into the master equation is not entirely trivial, as the derivation of the Lindblad master equation prominently relied on the system Hamiltonian being diagonal, which is typically not true when a driving term is introduced. The two conventional and common ways to incorporate the driving effects can each *potentially lead to different results*, depending on the parameter regime the system of interest is in. In Sec. II of this paper we review these two different approaches, and discuss their respective weaknesses and pitfalls. We then introduce a generalized approach in Sec. III, which unifies the previous treatments and extends the range of validity of

the quantum master equation. This more inclusive treatment is similar in essence to the equations derived in Ref. [11], whose main emphasis was the thermodynamics of the open system. We explore the consequences of using the more general approach, when is it superior compared to the more specialized schemes, what are the appropriate limits in which our approach converges with these schemes, and importantly, qualitative behavior which may obtained only using the generalized treatment. These include anomalous time evolution of the system coherence, population inversion in unusual regimes, and peculiar structure in the resonance fluorescence spectrum. The latter, which we study extensively in Sec. IV, was not previously considered in the context of the generalized master equation, though it appears to be quite relevant in distinguishing between different regimes. We also discuss the relevance of our results to recent experiments on quantum dots coupled to optical cavities [12–15] and single-electron paramagnetic resonance [16–18] (a full analysis of the latter type of systems was the subject of our recent work [19]). The latter is accessible in our approach, contrary to that of Ref. [11], as we further generalize the nature of the bath itself, and allow it to be out of thermal equilibrium. Lastly, in Sec. V we show when the proposed treatment may break down, an issue that was not previously fully examined. We summarize our findings in the Conclusions, Sec. VI. Appendix A details the derivation of our generalized master equation, while Appendix B elaborates on the calculation of two-time correlation functions.

II. DRIVEN OPEN SYSTEM

For the sake of clarity, but without loss of generality, we will focus our discussion on two-level systems, or "qubits." Prior to adding the driving term we have the Hamiltonian

$$H = H_S^0 + H_B + H_I, \tag{2}$$

with $H_S^0 = -\frac{1}{2}\omega_0\sigma_z$ (such that the ground state has $\sigma_z = +1$), H_B being the bath Hamiltonian, and the interaction $H_I = (a_x\sigma_x + a_y\sigma_y + a_z\sigma_z)\hat{B}$, where the σ's are Pauli matrices operating in the qubit Hilbert space, $\hat{B}$ is some bath operator (assuming different bath operators couple to each Pauli matrix does not lead to essential modifications [19]) which commutes with the qubit Pauli operators, and we henceforth set $\hbar = 1$. In this simple two-level scenario, the quantum jump operators in the dissipator are σ_-, σ_+, and σ_z. The corresponding rates will be denoted by $\gamma_\downarrow$, $\gamma_\uparrow$, and γ_0, respectively. These can be calculated from the bath spectral function as

$$\gamma_\downarrow \equiv \left(a_x^2 + a_y^2\right)K(\omega_0), \tag{3a}$$

$$\gamma_\uparrow \equiv \left(a_x^2 + a_y^2\right)K(-\omega_0), \tag{3b}$$

$$\gamma_0 \equiv a_z^2 K(0), \tag{3c}$$

with $K(\nu) \equiv \frac{1}{2}\,\mathrm{Re}\{\int_0^\infty d\tau\, e^{i\nu\tau}\langle\hat{B}(\tau)\hat{B}(0)\rangle_B\}$, where $\langle\cdot\rangle_B$ denotes an expectation value calculated in the bath's stationary state, which is unaffected by the system in the Born approximation, and will henceforth be assumed to be a thermal state at temperature T (we take the Boltzmann constant $k_B = 1$). The rate calculations are equivalent to Fermi's golden rule, as the imaginary parts of the bath correlation function contribute only a Lamb shift to H_S, not affecting the dissipative dynamics. Eq. (1) thus leads to decay and decoherence of the system, governed by these rates. Note that the secular approximation would now amount to the assumption that ω_0 is much greater than all γ's.

The effects of driving can be best understood by considering continuous periodic driving, which couples the ground and excited states of the two-level system. It can be written as an additional time-dependent term in the system Hamiltonian $H_S = H_S^0 + H_D$, with

$$H_D = \frac{\Omega}{2}(e^{i\omega_d t}\sigma_+ + e^{-i\omega_d t}\sigma_-), \tag{4}$$

where Ω is the driving amplitude, $\omega_d \equiv \omega_0 + \delta\omega$ is the driving frequency ($\delta\omega$ being the detuning), and we also define the generalized Rabi frequency $\omega \equiv \sqrt{\Omega^2 + \delta\omega^2}$. We assume a circularly polarized driving field, or else we keep only its components which appear in Eq. (4), i.e., the rotating-wave approximation (RWA) [20], justified for $\Omega \ll \omega_0, \omega_d$.

As the prescription for deriving Eq. (1) heavily relies on the system Hamiltonian being diagonal and time independent, the incorporation of such a driving term into the open quantum system framework is not entirely trivial. There are two common methods of introducing the driving effects into the Lindbladian master equation, which mainly differ in when the driving term is taken into account, as illustrated in Fig. 1 and described in the following.

A. Laboratory frame approach

In this approach the dissipative term in (1) is assumed to be the same as with H_S^0, and H_D in Eq. (4) is plugged into the commutator term. In other words, the driving is simply taken as an additional part of the system Hamiltonian [see Fig. 1(a)]. This procedure, of inserting the driving Hamiltonian "after the fact," i.e., deriving the dissipative master equation and subsequently changing H_S, *is perturbative in* Ω, meaning we would expect it to be appropriate only when Ω, or more accurately ω, is small compared to other relevant energy scales of the system, i.e., when

$$\omega \ll \omega_{\mathrm{bath}},\ T \ll \omega_d, \tag{5}$$

with the energy scale ω_{bath} defined as the typical scale over which $K(\nu)$ remains relatively constant around ω_d, while the temperature T plays a similar role around $\nu = 0$, e.g., in equilibrium detailed balance implies $K(\pm\omega) = K(0)(1 \pm \frac{\omega}{T})$ for $\omega \ll T$. The meaning of ω_{bath} can be illustrated through an example of a Lorentzian spectral density $K(\nu) \propto \frac{\gamma}{\gamma^2+(\nu-\nu^*)^2}$, peaked around some frequency ν^*, and having a width γ, e.g., a weakly coupled cavity mode [14]. Expanding $K(\omega_d \pm \omega)$ to first order in ω around ω_d, one finds

$$K(\omega_d \pm \omega) \approx K(\omega_d)\left(1 \pm 2\frac{\omega}{\omega_{\mathrm{bath}}}\right), \tag{6}$$

where $\omega_{\mathrm{bath}} = \omega_d - \nu^*$, and we have assumed $\gamma \ll |\omega_{\mathrm{bath}}|$.

Representing the system reduced density matrix as

$$\rho \equiv \begin{pmatrix} 1-n & \alpha \\ \alpha^* & n \end{pmatrix} = \frac{1}{2} + \frac{1-2n}{2}\sigma_z + \alpha^*\sigma_- + \alpha\sigma_+, \tag{7}$$

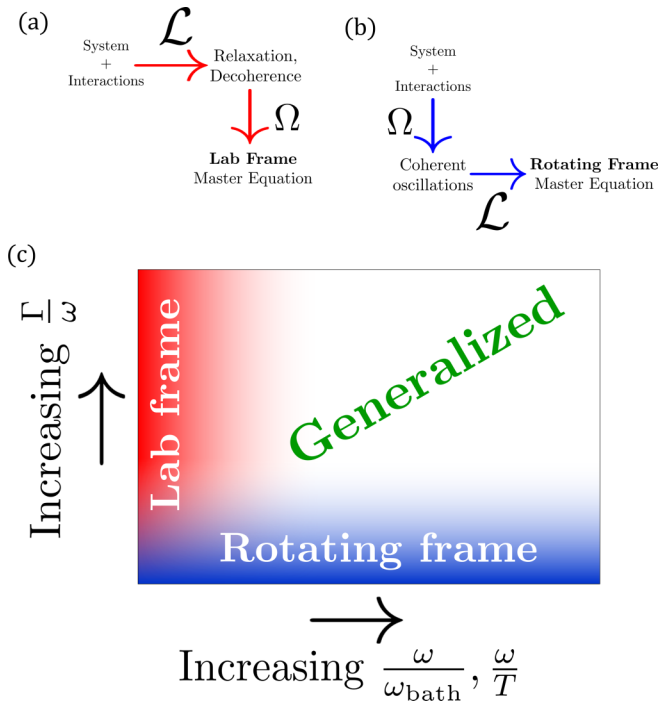

FIG. 1. Deriving the master equation for a driven open quantum system in two different ways. (a) In the laboratory frame approach, one first derives the non-driven Lindblad equation, and then introduces driving to the coherent dynamics. (b) By including the driving in the system Hamiltonian, and only then deriving the dissipative time evolution (making a secular approximation with respect to the driving terms), the rotating-frame approach leads to another distinct form of the master equation. (c) Schematic description of the range of validity of each of these treatments. Intensity of blue and red signifies how suitable the laboratory and rotating-frame approaches are, respectively, in those areas of parameter space. For $\Gamma \ll \omega \ll \omega_d$, the rotating-frame approach is adequate, while for $\omega \ll \omega_{\text{bath}}, T \ll \omega_d$ (causing only a small modification of the rates), the laboratory frame is better suited. Some overlap is apparent, but a region where both approaches are found wanting can only be be properly addressed by the proposed generalized approach.

the master equation is fully described by (in an interaction frame rotating with frequency ω_d)

$$\frac{d}{dt}n = -(\gamma_\downarrow + \gamma_\uparrow)n + \gamma_\uparrow - i\Omega\frac{\alpha - \alpha^*}{2}, \tag{8a}$$

$$\frac{d}{dt}\alpha = -(\tilde{\gamma} + i\delta\omega)\alpha - i\Omega\left(n - \frac{1}{2}\right), \tag{8b}$$

with $\tilde{\gamma} \equiv \frac{\gamma_\downarrow+\gamma_\uparrow}{2} + 2\gamma_0$. The more commonly known decay times characterizing the evolution of the qubit are then $\frac{1}{T_1} = \gamma_\downarrow + \gamma_\uparrow$, $\frac{1}{T_2^*} = 2\gamma_0$, and $\frac{1}{T_2} = \frac{1}{2T_1} + \frac{1}{T_2^*}$. This "laboratory frame" approach is popular mainly in atomic physics [21,22] and quantum optics [23], where the amplitude of the driving field may indeed be several orders of magnitude weaker compared to the qubit energy scale. This result is better known as the famous Bloch equations [24], which are entirely equivalent to (8a) and (8b) using the proper definitions.

B. Rotating-frame approach

Unlike the laboratory frame approach, the rotating-frame approach does take into account the effects of stronger driving on the dissipator. Here, the full system Hamiltonian is diagonalized first, and only then the Lindblad formalism takes place in the usual way [Fig. 1(b)]. This approach is most common in solid-state systems, e.g., superconducting qubits [25–27], where the driving cannot be dealt with in a perturbative manner.

Upon applying a transformation to a rotating frame by defining the unitary operator $U \equiv e^{-\frac{i\omega_d t}{2}\sigma_z}$ and transforming $H \to UHU^\dagger - iU\dot{U}^\dagger$, so as to eliminate the time dependence in H_D, and then diagonalizing the system Hamiltonian in this rotating frame, one arrives at the transformed Hamiltonian

$$\tilde{H} = \tfrac{1}{2}\omega\sigma_z + \tilde{H}_I + H_B. \tag{9}$$

A key factor here is the modification of the system-bath interaction Hamiltonian by the rotation U and by diagonalizing the system Hamiltonian. In the frame of Eq. (9), defining $\tilde{\rho} \equiv \left(\begin{smallmatrix} d & x \\ x^* & u \end{smallmatrix}\right)$ with $d = 1 - u$ yields the Lindblad master equation

$$\frac{d}{dt}u = -(\kappa_\uparrow + \kappa_\downarrow)u + \kappa_\uparrow, \tag{10a}$$

$$\frac{d}{dt}x = -\left(\frac{\kappa_\uparrow + \kappa_\downarrow}{2} + \kappa^* + i\omega\right)x, \tag{10b}$$

with rates defined as

$$\kappa_\uparrow = \frac{(\sin\beta - 1)^2}{4}\Gamma_\downarrow(1-\epsilon) + \frac{(\sin\beta + 1)^2}{4}\Gamma_\uparrow(1+\epsilon_e) + \cos^2\beta\Gamma_-^z, \tag{11a}$$

$$\kappa_\downarrow = \frac{(\sin\beta + 1)^2}{4}\Gamma_\downarrow(1+\epsilon) + \frac{(\sin\beta - 1)^2}{4}\Gamma_\uparrow(1-\epsilon_e) + \cos^2\beta\Gamma_+^z, \tag{11b}$$

$$\kappa^* = 2\sin^2\beta\Gamma_0^z + \frac{\cos^2\beta}{2}(\Gamma_\downarrow + \Gamma_\uparrow), \tag{11c}$$

where $\tan\beta \equiv \frac{\delta\omega}{\Omega}$, $\Gamma_\downarrow \equiv (a_x^2 + a_y^2)K(\omega_d)$, $\Gamma_\uparrow \equiv (a_x^2 + a_y^2)K(-\omega_d)$, $\Gamma_0^z = \gamma_0$, $\Gamma_\pm^z \equiv a_z^2 K(\pm\omega)$, and ϵ, ϵ_e are defined by a first order in ω expansion of the spectral density, $K(\omega_d \pm \omega) = K(\omega_d)[1 \pm \epsilon]$, and $K(-\omega_d \pm \omega) = K(-\omega_d)[1 \pm \epsilon_e]$. One typically expects $\epsilon, \epsilon_e \sim \omega/\omega_{\text{bath}}$. This approach evidently gives rise to a much richer landscape of rates governing the dissipation, with more bath spectral components appearing in the dissipator. However, an important key distinction of this approach compared to the laboratory frame is that in the transition from Eq. (9) to (10a) and (10b), we used a *secular approximation with regards to* ω, i.e., demanding

$$\Gamma_{\uparrow/\downarrow}, \Gamma_{0/\pm}^z \ll \omega \ll \omega_d. \tag{12}$$

In deciding which of the presented approaches to use when interested in the time evolution of a driven open quantum system, one must examine the validity of (5) or (12) [see Fig. 1(c)]. Although in some cases at least one of the assumptions may be appropriate, there are scenarios in which both are inadequate and will inevitably compromise the validity of the calculated dynamics.

III. A GENERALIZED APPROACH

A more inclusive *generalized approach*, where the aforementioned extra assumptions are not necessary, may be obtained by following the rotating frame method, and omitting the final secular approximation. Thus, the only assumption is that the bare qubit frequency ω_0 and the drive frequency ω_d are much larger than all other energy scales. This introduces additional nonsecular terms into the master equation for $\frac{d}{dt}\tilde{\rho}$, which in the rotating frame are time dependent with oscillatory factors going as $e^{\pm i\omega t}$ and $e^{\pm 2i\omega t}$ (see Appendix A). Then, by performing a unitary transformation $\rho \to e^{-i\tilde{H}_S t}\rho e^{i\tilde{H}_S t}$ (where $\tilde{H}_S = \frac{1}{2}\omega\sigma_z$), we eliminate these undesirable time dependencies. We find

$$\begin{aligned}\frac{d}{dt}n = &-n[\Gamma_\downarrow(1+\epsilon\sin\beta)+\Gamma_\uparrow(1+\epsilon_e\sin\beta)]\\ &+\Gamma_\uparrow(1+\epsilon_e\sin\beta)-i\Omega\frac{\alpha-\alpha^*}{2}\\ &-\frac{\alpha+\alpha^*}{2}\cos\beta\frac{\Gamma_\downarrow\epsilon+\Gamma_\uparrow\epsilon_e}{2},\end{aligned} \tag{13}$$

$$\begin{aligned}\frac{d}{dt}\alpha = &-\alpha(\tilde{\Gamma}+i\delta\omega)-i\Omega\left(n-\frac{1}{2}\right)\\ &+\left(n-\frac{1}{2}\right)\sin\beta\,\cos\beta\left(\Gamma_+^z+\Gamma_-^z-2\Gamma_0^z\right)\\ &-\frac{\Gamma_\downarrow\epsilon-\Gamma_\uparrow\epsilon_e}{4}\cos\beta-\frac{\Gamma_+^z-\Gamma_-^z}{2}\cos\beta,\end{aligned} \tag{14}$$

with $\tilde{\Gamma} \equiv \frac{\Gamma_\downarrow}{2}(1+\epsilon\sin\beta)+\frac{\Gamma_\uparrow}{2}(1+\epsilon_e\sin\beta)+(\Gamma_+^z+\Gamma_-^z)\cos^2\beta+2\Gamma_0^z\sin^2\beta$. Equations (13) and (14) are the main result of this paper. One immediately recognizes that taking the approximations $K(\pm\omega_d\pm\omega)\to K(\pm\omega_0)$ and $K(\pm\omega)\to K(0)$, leading to $\epsilon=\epsilon_e=0$ and $\Gamma_+^z=\Gamma_-^z=\Gamma_0^z$, recovers the laboratory frame equations (8a) and (8b). This approximation indeed requires the generalized Rabi frequency to be small enough, in the sense of Eq. (5).

As a first example of the difference in the resulting open system dynamics when employing the various approaches, the time evolution of the driven qubit is numerically calculated and shown in Fig. 2 for each approach. As the calculations take place in a regime where neither (5) nor (12) are adequate (the generalized Rabi frequency is comparable to the decay rates, and we introduce finite asymmetry ϵ to the spectral components that determine the rates), we expect the qubit "trajectory" in the previous Lindbladian approaches to deviate from our less restrictive general calculation. While the differences in $n(t)$, the excited-state population, are moderate, the departure from the generalized result in the evolution of the coherence α, for both the laboratory and rotating frame approaches, is much more dramatic, both in terms of the steady-state value and the evolution toward it. This component of the density matrix is commonly the one of most interest for quantum devices.

The importance of the spectral asymmetry of K around the driving frequency ω_d and the dc component already becomes clear at the steady-state level for n, namely, the possibility of *population inversion in the qubit*, even in the regime $\Gamma_\uparrow < \Gamma_\downarrow$ (see Fig. 3). While this effect is possible in the rotating-frame approach, it is completely absent from the laboratory frame one. The generalized treatment allows us to explore such a remarkable effect without requiring any unnecessary assumptions on the size of the decay rates relative to ω. Thus, even in systems where Eq. (12) is somewhat inadequate, population inversion may be detected as a possible signature of spectral asymmetry.

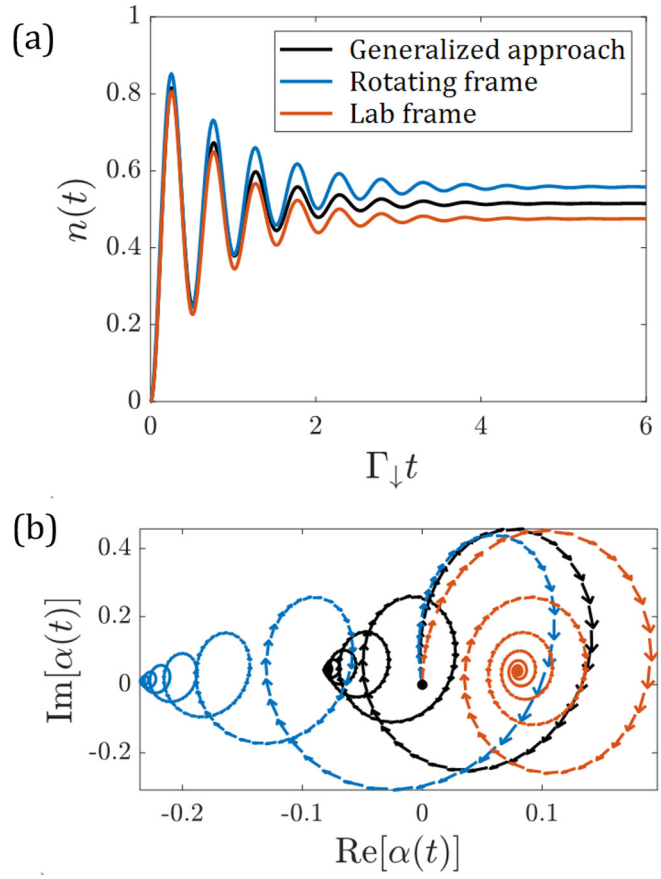

FIG. 2. Time evolution of the density matrix components under the three different approaches discussed: laboratory frame (red), rotating frame (blue), and the generalized approach (black). (a) The time evolution of the excited-state population. (b) Evolution of the off-diagonal component α in the complex plane, beginning at $(0,0)$ (large black dot) and following the direction of the arrows. Initially, the qubit is in the pure two-level ground state $[n(0)=0, \alpha(0)=0]$, and the parameters used are $\Omega = 12\Gamma_\downarrow$, $\delta\omega = 3\Gamma_\downarrow$, $\Gamma_0^z = \frac{1}{2}\Gamma_\downarrow$, $\Gamma_\pm^z = \Gamma_0^z(1\pm\frac{1}{2})$, $\epsilon = 0.1$, and $\Gamma_\uparrow = \epsilon_e = 0$.

IV. RESONANCE FLUORESCENCE

An interesting quantity often measured in experiments is the correlation function

$$g(\nu) \equiv \int_{-\infty}^{\infty} d\tau\, e^{i\nu\tau}\langle\sigma_-(t_0)\sigma_+(t_0+\tau)\rangle, \tag{15}$$

representing resonance fluorescence [28,29], i.e., the cross section for inelastic scattering of photons near resonance. It typically features the Mollow triplet of peaks at the original frequency ω_d and at the dressed frequencies $\omega_d\pm\omega$. By utilizing the quantum regression theorem [30], we per-

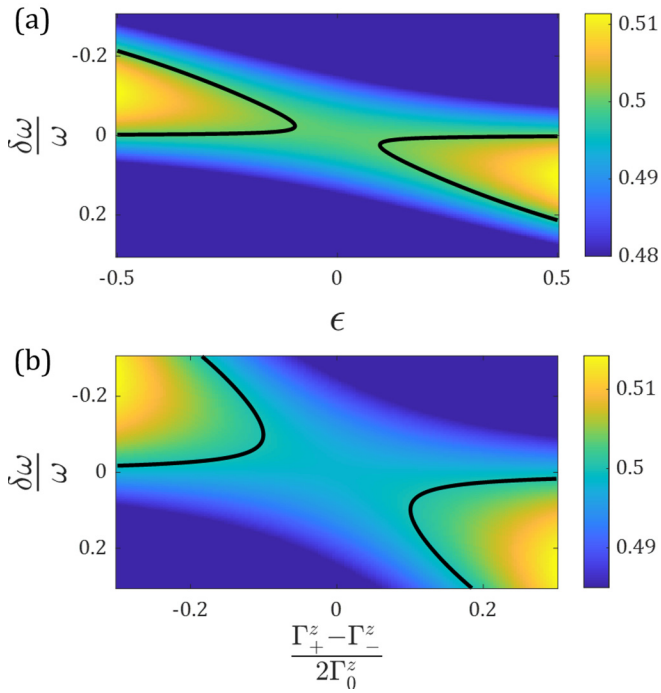

FIG. 3. Steady-state excited-state qubit population n in the presence of spectral asymmetry of the bath correlation function K. (a) n as a function of ϵ and detuning, with $\Gamma^z_0 = \frac{1}{20}\Gamma_\downarrow$ and $\Gamma^z_+ = \Gamma^z_- = \Gamma^z_0$. (b) n as a function of the longitudinal asymmetry $\frac{\Gamma^z_+-\Gamma^z_-}{2\Gamma^z_0}$ and detuning, with $\epsilon = 0$, $\Gamma^z_0 = \Gamma_\downarrow$, and $\Gamma^z_+ + \Gamma^z_- = 2\Gamma^z_0$. The areas within the solid black lines are where population inversion occurs, $n > \frac{1}{2}$, and the color scale is chosen as to accentuate the effect. Other parameters used: $\Gamma_\uparrow = \epsilon_e = 0$, $\Omega = 25\Gamma_\downarrow$.

form calculations with the three different approaches (see Appendix B) in two distinct parameter regimes, distinguished by the size of the driving amplitude Ω. In the first regime, Ω is sufficiently large such that it causes a significant shift in $\Gamma^z_\pm$ away from Γ^z_0, making (5) inadequate. This results in the asymmetry of the triplet shown in Fig. 4(a). In this large-Ω regime the rotating-frame approach approximates well the generalized one, while the laboratory frame is not reliable as all the effects of the driving on the dissipator are neglected. In the other regime, Ω is smaller and comparable in size to the decay rates, such that (12) is violated. In that case, the rotating-frame approach is not applicable since the additional secular approximation is not well justified. This discrepancy is clearly visible in Fig. 4(b), where the laboratory frame result matches fairly well the generalized one.

The generalized approach, as explained before, allows for a more complete description of the dynamics in both of these extreme regimes, and in all the parameter ranges in-between. The calculation presented in Fig. 4(c) is an example of such an intermediate regime. In this scenario the different parameters are chosen such that ω is comparable with both the decay rates *and* the energy scales determining the spectral asymmetry ω_{bath} and T. In Fig. 4(c) the complex structure of the two side peaks is considerably misrepresented by either the laboratory or rotating-frame treatments. The asymmetric generalized result has significantly greater range of applicability in the chosen parameter regime, and is able to capture the interplay

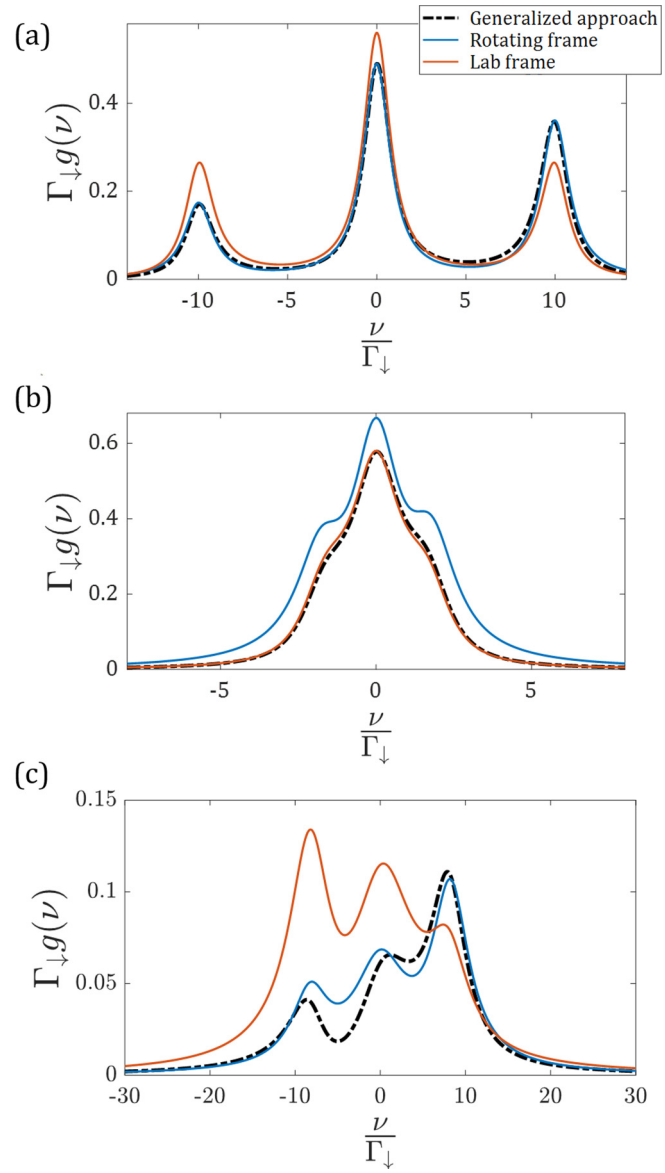

FIG. 4. $g(\nu)$ calculated using the different approaches discussed: laboratory frame (red), rotating frame (blue), and generalized approach (black) for different parameter sets: (a) $\Omega = 1.8\Gamma_\downarrow$, $\Gamma^z_0 = 0.2\Gamma_\downarrow$, $\Gamma^z_\pm = \Gamma^z_0(1 \pm \frac{\omega}{T})$, $T = 12.5\Gamma_\downarrow$, and $\delta\omega = \Gamma_\uparrow = \epsilon_e = \epsilon = 0$. (b) Same as (a), except for $\Omega = 10\Gamma_\downarrow$. (c) $\Omega = 8\Gamma_\downarrow$, $\delta\omega = -2\Gamma_\downarrow$, $\Gamma^z_0 = 2\Gamma_\downarrow$, $\Gamma^z_+ = 3\Gamma_\downarrow$, $\Gamma^z_0 = 0.4\Gamma_\downarrow$, and $\Gamma_\uparrow = \epsilon_e = \epsilon = 0$.

between the detuning, which "favors" lower frequencies since it is negative, and the spectral asymmetry, having the opposite effect due to $\Gamma^z_+ > \Gamma^z_0$.

Interestingly, the resonance fluorescence spectra of semiconductor quantum dots in optical cavities, which comprise effective two-level systems, have been extensively measured [12–15,31]. Our generalized approach is particularly relevant to such experiments since (i) the driving amplitudes used are typically not much greater than the dissipative energy scale which determines the linewidths, such that the rotating-frame approach is somewhat inadequate, and (ii) the spectral density of the qubit bath is heavily influenced by the proximity of a cavity mode to the quantum dot resonance. This is especially important in the limit of weak coupling to a cavity, where

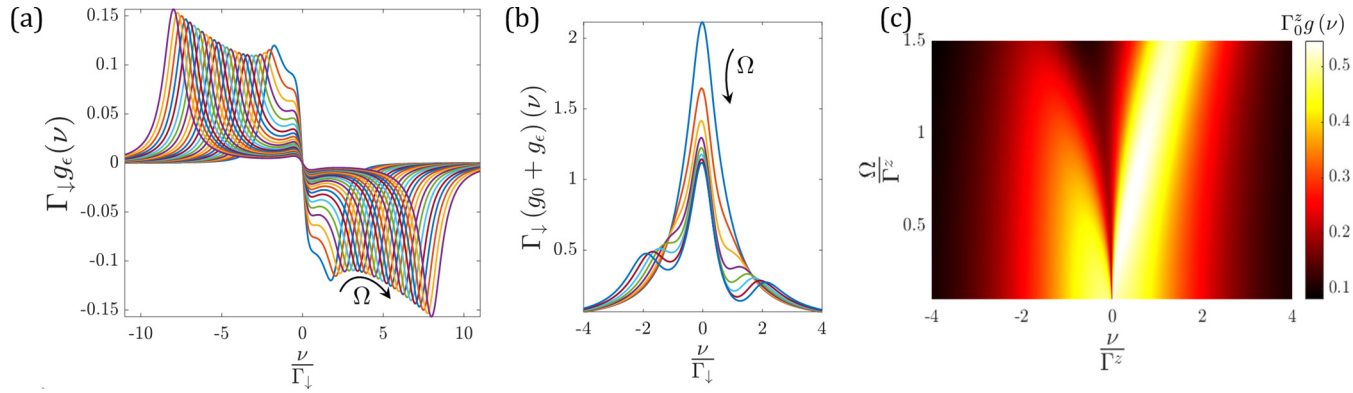

FIG. 5. Relevant experimental signatures in regimes where only the generalized approach is free from inadequate approximations on the system dynamics. (a) The asymmetric correction to the resonance fluorescence spectrum $g_\epsilon(\nu)$, calculated on resonance for zero longitudinal coupling. The values of $\frac{\Omega}{\Gamma_\downarrow}$ we use vary from 2 to 8, in steps of 0.25 (the direction of increasing Ω is indicated by an arrow). (b) The full corrected line shape in the regime $\Omega \sim \Gamma_\downarrow$. $\frac{\Omega}{\Gamma_\downarrow}$ varies from 0.5 to 2 with steps of 0.2 (the direction of increasing Ω is indicated by an arrow). In (a), (b) we use $\epsilon \approx \frac{\omega}{\omega_{\text{bath}}}$, with $\omega_{\text{bath}} = -20\Gamma_\downarrow$. (c) $\Gamma_0^z g(\nu)$ in the large dephasing regime $\frac{1}{T_1} \ll \Omega \lesssim \frac{1}{T_2}$ on resonance, with different driving amplitudes. Here, we use the asymmetry parameter $\Delta = 0.4$.

the loss rate of the cavity is much higher than the coupling constant to the quantum dot (see, e.g., Ref. [14]). In that case, instead of using the full Jaynes-Cummings model to account for the cavity mode, we can incorporate it as a bath with transverse coupling and a peaked spectral density, arriving at the situation described by Eq. (6), i.e., $\epsilon \approx \frac{\omega}{\omega_{\text{bath}}}$. This can make the spectral functions $K(\pm\omega_d - \omega)$, $K(\pm\omega_d)$, and $K(\pm\omega_d + \omega)$ significantly different from one another even when $\omega \ll \omega_d$, and lead to an apparent asymmetry in the resonance fluorescence spectrum, similarly to Fig. 4. For the simplified case of zero longitudinal coupling and $\Gamma_\uparrow = 0$, the resonance fluorescence spectrum on resonance is given by $g = g_0(\nu) + g_\epsilon(\nu) + \mathcal{O}(\epsilon^2)$, with $g_0(\nu)$ being the laboratory frame result, and ν is the scattered frequency in the rotating frame (i.e., it is $\nu + \omega_d$ in the laboratory frame). The result on resonance $\delta\omega = 0$ is

$$g_0(\nu) = 4\Gamma_\downarrow \frac{\Gamma_\downarrow^2(\Gamma_\downarrow^2+\nu^2)(\Gamma_\downarrow^2+4\nu^2) + 2\Omega^2((\Gamma_\downarrow^2+\Omega^2)^2 - (\Gamma_\downarrow^2+2\Omega^2)\nu^2 + 4\nu^4)}{(\Gamma_\downarrow^2+4\nu^2)(\Gamma_\downarrow^2+2\Omega^2)[\Gamma_\downarrow^2(\Gamma_\downarrow^2+4\Omega^2+5\nu^2) + 4(\nu^2-\Omega^2)^2]}, \tag{16}$$

$$g_\epsilon(\nu) = 2\epsilon\Gamma_\downarrow\Omega\nu \frac{\Gamma_\downarrow^2(13\Gamma_\downarrow^2+11\Omega^2) + 4\nu^2(\Gamma_\downarrow^2+3\Omega^2)}{(\Gamma_\downarrow^2+4\nu^2)(\Gamma_\downarrow^2+2\Omega^2)[\Gamma_\downarrow^2(\Gamma_\downarrow^2+4\Omega^2+5\nu^2) + 4(\nu^2-\Omega^2)^2]}. \tag{17}$$

The correction to the resonance fluorescence spectrum is valid for arbitrary $\frac{\Omega}{\Gamma_\downarrow}$ within the generalized treatment, and thus could not be reliably obtained by the usual rotating-frame treatment. Notice that $g_\epsilon(\nu)$ will lead to an asymmetry, due to it being an odd function of ν [see Fig. 5(a)]. For $\Omega \gg \Gamma_\downarrow$, g_ϵ is peaked mainly around $\pm\Omega$, yet a crossover into a regime where only our generalized approach is valid is clearly apparent when Ω is decreased. For this smaller driving amplitude regime, the asymmetry may begin to be visibly pronounced in the central peak as well, as can be seen in Fig. 5(b). The lower driving amplitude regime shows some resemblance to the results presented in Ref. [14] [lower curves in Fig. 2(a)].

This asymmetric effect is in line with the measurements made in Refs. [13–15], which showed an asymmetry which grows with the driving amplitude. In Ref. [14], a triplet asymmetry of 15% was reported, consistent with the proximity to the cavity mode $\frac{\omega}{\omega_{\text{bath}}} \sim 0.1$–$0.3$. A small amount of asymmetry could also be noticed in the central triplet peak in some of the plots of Ref. [14] with smaller Ω, in agreement with our theoretical predictions. The possible effect of the cavity was actually pointed out in Ref. [32]. However, that work utilizes an analog of the rotating-frame approach, *which is not entirely justified* in this particular experimental regime, though it provides a decent qualitative description. In Ref. [12] the Rabi frequency is even tuned all the way down below T_2^{-1}, prompting its authors to employ the restrictive laboratory frame approach. Thus, we conclude that the generalized approach is needed to account for the behavior of common cavity-coupled quantum dots, as it is the only one capturing the asymmetric features without imposing inadequate approximations.

We note that the so-called excitation-induced dephasing (EID) effect may also be captured using our generalized approach. By expanding, e.g., $K(\omega_d \pm \omega)$ to second order in $\frac{\omega}{\omega_{\text{bath}}}$, additional terms are added to our master equations (13) and (14), among them is the change of the dephasing rate $\tilde{\Gamma} \to \tilde{\Gamma} + \frac{\Gamma_\downarrow}{4}\upsilon$, with $K(\omega_d \pm \omega) \approx K(\omega_d)(1 \pm \epsilon + \upsilon)$. Now, $\upsilon \propto (\frac{\omega}{\omega_{\text{bath}}})^2$, i.e., the dephasing increases like Ω^2. We have verified numerically that the linewidths of the Mollow triplet taken with finite υ increase linearly with Ω^2, similar to experimental results in comparable regimes [14,33]. Similarly to the effect

of ϵ, this behavior exists also in the rotating-frame regime, and our proposed treatment allows one to dependably obtain it in a broader parameter regime, namely, weaker driving.

To conclude this section, let us turn to an important regime of interest, especially relevant in the context of single-spin electron paramagnetic resonance (EPR) experiments [16–18], where $\frac{1}{T_1} \ll \Omega \lesssim \frac{1}{T_2}$, i.e., very small decay rates yet large dephasing coupling strength, which is comparable to or exceeds the Rabi energy scale. The rotating-frame approach is ruled out immediately in such a regime. We have recently demonstrated that experimental results for the aforementioned EPR systems cannot be accounted for by the standard laboratory frame approach, and that our generalized treatment enables capturing the important observed features when taking into account the out-of-equilibrium nature of the bath the system is coupled to, i.e., the electronic reservoirs [19]. As an example for what is missed by the laboratory frame approach, we consider $\Gamma_{\uparrow/\downarrow} = 0$, $\delta\omega = 0$, and $\Gamma^z_\pm \equiv \Gamma^z_0(1 \pm \Delta\frac{\omega}{\Gamma^z_0})$, i.e., we only consider the first order in ω correction to the laboratory frame rates. In equilibrium, detailed balance dictates $\frac{\Delta}{\Gamma^z_0} \approx \frac{1}{T}$. We calculate the spectral function

$$g(\nu) = \frac{\Gamma^z_0}{\left(2\Gamma^z_0\right)^2 + \nu^2}\left[1 - \left(\frac{\Delta\Omega}{\Gamma^z_0}\right)^2\right] + \nu^2 \frac{\Gamma^z_0}{\left(2\Gamma^z_0\right)^2\nu^2 + (\nu^2 - \Omega^2)^2} + \nu\frac{\Delta\Omega}{\Gamma^z_0}\frac{\Omega\Gamma^z_0}{\left(2\Gamma^z_0\right)^2\nu^2 + (\nu^2 - \Omega^2)^2}. \quad (18)$$

For $\Delta = 0$, we have the usual Mollow triplet with peaks at $\nu = 0, \pm\Omega$ for large driving amplitudes. As Ω decreases, this latter term overshadows the first one, leading to an apparent "doublet" structure, with a sharp dip at zero. The third term in Eq. (18) is an asymmetry term, similar to the one in Eq. (17). Figure 5(b) shows the shape of the spectrum with varying Ω, far from the rotating-frame range of validity. It features clear asymmetry absent from the laboratory frame approach.

V. APPLICABILTY OF THE GENERALIZED QUANTUM MASTER EQUATION

As discussed above, our generalized master equations (13) and (14) are not of the standard Lindblad form, unlike either laboratory frame or rotating-frame master equations. Keeping the important Markovian approximation, as we still do in the generalized scheme, means that the master equation now takes the Redfield form [34], *which does not guarantee that the density matrix remains positive semidefinite* [35,36], though the Hermiticity and normalization ($\mathrm{Tr}\{\rho\} = 1$) are still preserved. Therefore, when making use of the proposed generalized approach, one should understand when it might become invalid, resulting in, e.g., "negative probabilities" (indicating unphysical results [35]). It should be pointed out, however, that a master equation which has the Lindblad form does not necessarily preclude nonphysical behavior of the open quantum system [37].

Since the trace of the density matrix is fixed at unity, as just stated, for a two-level system its positivity is determined by its determinant: a negative determinant would immediately signal that one of the density matrix eigenvalue is negative (in addition to the second eigenvalue being larger than 1). The determinant can simply be written as

$$\det\rho = n(1-n) - |\alpha|^2. \quad (19)$$

We note that the possibility of $n < 0$ or $n > 1$ is also captured by a negative density matrix determinant, as evident by (19). We find that although Eqs. (8a) and (8b) in principle allow these values of n, in practice one requires unphysically large asymmetry parameters (ϵ, Δ) for this to occur.

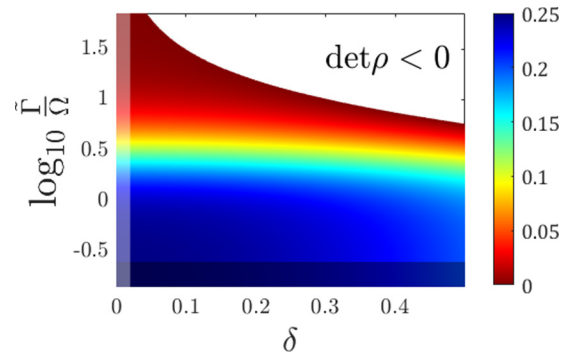

FIG. 6. Determinant of the steady-state ($t \to \infty$) density matrix in different regimes. The blank area is where the determinant is negative, and therefore the solution is unphysical. The brighter area to the left approximately corresponds to the rotating-frame regime, whereas the darker area at the bottom is properly captured by the laboratory frame approach. Throughout this calculation we used $\Gamma^z_0 = 2\Gamma_\downarrow$, $\Gamma^z_\pm = \Gamma^z_0(1 \pm \delta)$, and $\delta\omega = \Gamma_\uparrow = \epsilon_e = \epsilon = 0$.

As an example, calculation of the determinant of ρ in its steady state is presented in Fig. 6. For illustrative purposes the departure from the laboratory frame regime is achieved by forcing an ω-independent asymmetry in the longitudinal rates, $\Gamma^z_\pm = \Gamma^z_0(1 \pm \delta)$, whereas a small driving amplitude Ω compared to the decay rates drives our master equation away from the rotating-frame regime of validity. Clearly, there exists a regime in parameter space where positivity is not maintained (or is close to being lost), yet this regime is far removed from the scenarios that were previously accessible under the approximations of the Lindbladian treatments. In other words, in the area between the bottom of Fig. 6 and its left-hand side, representing the rotating-frame and laboratory frame regimes, respectively, a significant amount of new ground is covered by the generalized approach, allowing a better understanding of the open system dynamics in intermediate regimes (as in Fig. 2).

We note that restoring density matrix positivity in Redfield-type master equations has been suggested to be possible [38] by dividing the time evolution of the system into two parts: at initial times the time evolution takes place with the full non-Markovian dynamics (leading to a more complex master equation which is harder to handle). After time t_b, which characterizes the bath relaxation time and thus the scale at which any memory effects in the bath decay, the unmodified Redfield time evolution is implemented. This can be thought of as sort of a "slippage" of the initial conditions for ρ. This sort of modification, however, cannot resolve the discrepancy

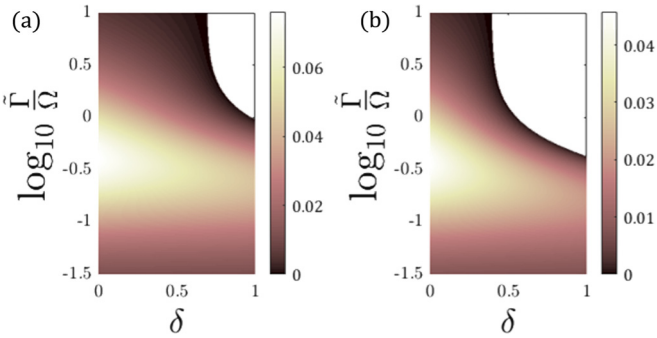

FIG. 7. Steady-state value of $\mathrm{Im}\{\alpha\}$ as a function of driving strength and longitudinal asymmetry. The blank areas represent $\mathrm{Im}\{\alpha\} < 0$, i.e., a negative power flow [Eq. (20)]. Similarly to Fig. 6, the bottom of each panel corresponds to the rotating-frame regime, while the laboratory frame approach better captures the leftmost $\delta = 0$ parts. (a) $\Gamma_\uparrow = \frac{1}{4}\Gamma_\downarrow$; (b) $\Gamma_\uparrow = \frac{1}{2}\Gamma_\downarrow$. Other parameters are kept constant at $\Gamma_0^z = 2\Gamma_\downarrow$, $\Gamma_\pm^z = \Gamma_0^z(1 \pm \delta)$, $\delta\omega = -\Gamma_\downarrow$, and $\epsilon_e = \epsilon = 0$.

shown in Fig. 6, as it only pertains to the *steady-state* density matrix, which is independent of initial conditions.

An additional criterion one may employ to determine the validity of our proposed treatment is the rate at which energy introduced to the system by the periodic drive is dissipated into the bath, which in the steady state is given by [11]

$$\mathcal{P} = \left\langle \frac{\partial}{\partial t} H_D \right\rangle = \hbar\omega_d \Omega\, \mathrm{Im}\{\alpha\}, \tag{20}$$

where terms varying as $e^{\pm 2i\omega_d t}$ were averaged to zero. Except for the anomalous regime $\Gamma_\uparrow > \Gamma_\downarrow$ (where the bath causes net excitation of the system), this quantity should remain nonnegative to ensure that energy flows from the drive through the qubit and into the bath. We find that for a combination of "red" detuned driving ($\delta\omega < 0$), finite $\frac{\Gamma_\uparrow}{\Gamma_\downarrow}$ ratio, and sufficient longitudinal asymmetry $\frac{\Gamma_+^z - \Gamma_-^z}{2\Gamma_0^z}$, a regime appears where the generalized treatment results in apparent negative power flow (see Fig. 7). However, once again, the region in parameter space where the generalized treatment breaks down is far from the reach of the previous approaches, and a substantial formerly mistreated part of this parameter space can now be more reliably accounted for.

VI. CONCLUSIONS

A more general approach for treating a driven open quantum system has been introduced and was shown to reduce to previous prevalent Lindblad approaches in some specialized limits. The Lindbladian treatments are limited in their applicability: one needs either the generalized Rabi frequency ω to be sufficiently small such that spectral properties of the bath do not change greatly under a shift of $\pm\omega$, or that this frequency is much larger than all the dissipation rates. The proposed treatment enables a seamless transition between these two regimes, and allows a better understanding of their connection to each other which was previously ambiguous, thus paving the way toward the analysis of open quantum systems occupying new areas of parameter space. In these previously unexplored parameter regimes, our proposed approach reveals, among other things, the intricate time-evolution behavior of the crucial coherence terms, possibilities for population inversion and EID even with intermediate driving amplitudes, and unique structure in the resonance fluorescence spectrum. The generalized approach we present in this work is free of the inapplicable approximations which plague the existing approaches.

We demonstrate the relevance of our approach to experiment on quantum dot qubits, where a crossover from the weak to the strong driving regimes may occur, and the spectral content of the bath is not trivial due to proximity to a cavity mode. We have shown that in such systems the cavity-distorted bath spectral density may lead to an asymmetry of the resonance fluorescence spectrum, even in the central peak, an effect observed in experiments yet theoretically inaccessible in either laboratory or rotating-frame regimes.

Our proposed treatment is also needed for appropriately analyzing single EPR experiments [19], in addition to other systems in the parameter regime $\frac{1}{T_1} \ll \Omega \lesssim \frac{1}{T_2}$. In such regimes, the Mollow triplet becomes a doublet, which becomes visibly asymmetric for low enough temperatures, or in certain out-of-equilibrium cases, as discussed in Ref. [19].

Furthermore, as the recent trend of combining devices from different disciplines and different regimes is gradually accelerating [39–42], the shift to a more unified perspective akin to the one presented in this work may be unavoidable. Based on the principles shown in this work, such an extension is straightforward, as our approach imposes way less restrictions in terms of the relations between different energy scales in the system.

ACKNOWLEDGMENTS

M.G. was supported by the Israel Science Foundation (Grant No. 227/15), the German Israeli Foundation (Grant No. I-1259-303.10), the US-Israel Binational Science Foundation (Grants No. 2014262 and No. 2016224), and the Israel Ministry of Science and Technology (Contract No. 3-12419). B.H. thanks stimulating discussions with A. Shnirman, G. Zaránd, and D. Cohen and acknowledges support by German-Israeli DIP project (Hybrid devices: Grant No. FO 703/2–1).

APPENDIX A: DERIVING THE GENERALIZED MASTER EQUATION

Starting from the driven Hamiltonian of a system coupled to a bath, we present here the full derivation of the master equations (13) and (14), and show that it generalizes the rotating-frame approach. The full Hamiltonian in the rotating frame with frequency ω_d is

$$H = \tfrac{1}{2}\delta\omega\sigma_z + \tfrac{1}{2}\Omega\sigma_x + H_B \tag{A1}$$

$$- \tfrac{1}{2}(a e^{i\omega_d t}\sigma_- + a^* e^{-i\omega_d t}\sigma_+ + a_z\sigma_z)\hat{B}, \tag{A2}$$

with $a = a_x + i a_y$. We can diagonalize the system part of this Hamiltonian by transforming $H \to \tilde{H} = S^{-1}HS$,

with ($\tan\beta \equiv \frac{\delta\omega}{\Omega}$)

$$S = \frac{1}{\sqrt{2}} \underbrace{\begin{pmatrix} \cos\frac{\beta}{2} + \sin\frac{\beta}{2} & -\cos\frac{\beta}{2} + \sin\frac{\beta}{2} \\ \cos\frac{\beta}{2} - \sin\frac{\beta}{2} & \cos\frac{\beta}{2} + \sin\frac{\beta}{2} \end{pmatrix}}_{\text{system subspace}} \otimes 1_{\text{bath subspace}}. \tag{A3}$$

Thus, we have $\tilde{H} = \frac{1}{2}\omega\sigma_z - (A_0 + A_1 + A_{-1})\hat{B} + H_B$, with

$$A_0 = \left(\frac{\sin\beta}{2}a_z + \frac{\cos\beta}{4}(a^* e^{-i\omega_d t} + a e^{i\omega_d t})\right)\sigma_z, \tag{A4a}$$

$$A_1 = \Lambda(t)\sigma_-, \tag{A4b}$$

$$A_{-1} = \Lambda^*(t)\sigma_+, \tag{A4c}$$

where $\Lambda(t) = \frac{\sin\beta - 1}{4}a^* e^{-i\omega_d t} + \frac{\sin\beta + 1}{4}a e^{i\omega_d t} - \frac{\cos\beta}{2}a_z$. Moving into the interaction picture of the system (made possible by the diagonalization of the system Hamiltonian), $A_{\pm 1}(t)$ pick up an additional $e^{\pm i\omega t}$ factor multiplying them. In this picture, the Markovian master equation reads as [34]

$$\frac{d}{dt}\tilde{\rho}(t) = \sum_{j,k=-1}^{1}\int_0^\infty ds\, C(s)[A_j(t-s)\tilde{\rho}(t), A_k^\dagger(t)] + \text{H.c.}, \tag{A5}$$

with $C(\tau) \equiv \text{Tr}_B\{\rho_B \tilde{B}(t)\tilde{B}(t-\tau)\}$ the bath correlation function. We may now plug the $A_j(\tau)$ operators in the master equation, decompose the system density matrix as $\tilde{\rho} = \frac{d+u}{2} + \frac{d-u}{2}\sigma_z + x\sigma_- + x^*\sigma_+$, and perform the integral over time s in (A5). Examination of (A4a)–(A4c) reveals that the only oscillation frequencies which can appear in the master equation are

$$0, \pm\omega, \pm 2\omega, \pm\omega_d, \pm(\omega_d \pm \omega), \pm 2\omega_d.$$

Keeping the RWA and the more general laboratory frame secular approximation allows us to discard terms oscillating with frequencies that are in the vicinity of ω_d or higher (we also assume $\omega_d, \omega_0 \gg \omega$), leading to an equation of the form

$$\frac{d}{dt}\tilde{\rho}(t) = \mathcal{D}_0 + \mathcal{D}_\omega + \mathcal{D}_{2\omega} + \text{H.c.} \tag{A6}$$

Substituting the rates we have defined in the main text, these terms read as

$$\begin{aligned}
\mathcal{D}_0 = &-\left(d\sigma_z + x^*\sigma_+\right)\left(\frac{(\sin\beta - 1)^2}{8}\Gamma_\downarrow(1-\epsilon) + \frac{(\sin\beta + 1)^2}{8}\Gamma_\uparrow(1+\epsilon_e) + \frac{\cos^2\beta}{2}\Gamma_-^z\right) \\
&+ (u\sigma_z - x\sigma_-)\left(\frac{(\sin\beta + 1)^2}{8}\Gamma_\downarrow(1+\epsilon) + \frac{(\sin\beta - 1)^2}{8}\Gamma_\uparrow(1-\epsilon_e) + \frac{\cos^2\beta}{2}\Gamma_+^z\right) \\
&- \left(x\sigma_- + x^*\sigma_+\right)\left(\sin^2\beta\Gamma_0^z + \frac{\cos^2\beta}{4}\left(\Gamma_\downarrow + \Gamma_\uparrow\right)\right),
\end{aligned} \tag{A7a}$$

$$\begin{aligned}
\mathcal{D}_\omega = &-e^{i\omega t} d\sigma_- \cos\beta\left(\frac{\sin\beta - 1}{4}\Gamma_\downarrow(1-\epsilon) + \frac{\sin\beta + 1}{4}\Gamma_\uparrow(1+\epsilon_e) - \sin\beta\Gamma_-^z\right) \\
&+ e^{-i\omega t} u\sigma_+ \cos\beta\left(\frac{\sin\beta + 1}{4}\Gamma_\downarrow(1+\epsilon) + \frac{\sin\beta - 1}{4}\Gamma_\uparrow(1-\epsilon_e) - \sin\beta\Gamma_+^z\right) \\
&- e^{-i\omega t}(\sigma_+ + x\sigma_z)\frac{\cos\beta}{2}\left(\frac{\sin\beta + 1}{4}\Gamma_\uparrow + \frac{\sin\beta - 1}{4}\Gamma_\downarrow - \sin\beta\Gamma_0^z\right) \\
&+ e^{i\omega t}\left(\sigma_- - x^*\sigma_z\right)\frac{\cos\beta}{2}\left(\frac{\sin\beta - 1}{4}\Gamma_\uparrow + \frac{\sin\beta + 1}{4}\Gamma_\downarrow - \sin\beta\Gamma_0^z\right),
\end{aligned} \tag{A7b}$$

$$\begin{aligned}
\mathcal{D}_{2\omega} = &\, e^{2i\omega t} x^*\sigma_-\left(\frac{\sin^2\beta - 1}{8}\Gamma_\downarrow(1-\epsilon) + \frac{\sin^2\beta - 1}{8}\Gamma_\uparrow(1+\epsilon_e) + \frac{\cos^2\beta}{2}\Gamma_-^z\right) \\
&+ e^{-2i\omega t} x\sigma_+\left(\frac{\sin^2\beta - 1}{8}\Gamma_\downarrow(1+\epsilon) + \frac{\sin^2\beta - 1}{8}\Gamma_\uparrow(1-\epsilon_e) + \frac{\cos^2\beta}{2}\Gamma_+^z\right),
\end{aligned} \tag{A7c}$$

where $\tilde{\rho} = \begin{pmatrix} d & x \\ x^* & u \end{pmatrix}$. Note that the master equations for the rotating-frame approach, Eqs. (10a) and (10b), are obtained by taking the secular approximation with regards to ω, i.e., $\mathcal{D}_\omega, \mathcal{D}_{2\omega} \to 0$, and moving out of the interaction picture. However, by keeping all these oscillating terms, we arrive at a more general form of $\frac{d}{dt}\tilde{\rho}$. Following the unitary transformation defined in the main text as $e^{i\tilde{H}_S t}$, we invert the diagonalization transformation S [Eq. (A3)], in order to find the master equation in the original laboratory frame $\rho = \begin{pmatrix} 1-n & \alpha \\ \alpha^* & n \end{pmatrix}$, using

$$n = \frac{1}{2} + \left(u - \frac{1}{2}\right)\sin\beta - \frac{x + x^*}{2}\cos\beta, \tag{A8a}$$

$$\alpha = \left(u - \frac{1}{2}\right)\cos\beta + \frac{x + x^*}{2}\sin\beta - \frac{x - x^*}{2}. \tag{A8b}$$

This allows us to retrieve the full generalized master equations in the main text, (13) and (14).

For the sake of completeness, we bring here the master equations for two limiting cases: (i) pure dephasing only, i.e., $a = 0$, which gives

$$\frac{d}{dt}n = -i\Omega\frac{\alpha-\alpha^*}{2}, \tag{A9a}$$

$$\frac{d}{dt}\alpha = -\alpha\left[(\Gamma_+^z+\Gamma_-^z)\cos^2\beta + 2\Gamma_0^z\sin^2\beta + i\delta\omega\right] + \left(n-\frac{1}{2}\right)\left[\frac{\sin 2\beta}{2}\left(\Gamma_+^z+\Gamma_-^z-2\Gamma_0^z\right) - i\Omega\right] - \frac{\cos\beta}{2}(\Gamma_+^z-\Gamma_-^z), \tag{A9b}$$

and (ii) purely radiative decay ($a_z = 0$), giving

$$\frac{d}{dt}\alpha = -\alpha\left(\frac{\Gamma_\downarrow}{2}(1+\epsilon\sin\beta)+\frac{\Gamma_\uparrow}{2}(1+\epsilon_e\sin\beta)+i\delta\omega\right) - i\Omega\left(n-\frac{1}{2}\right) - \frac{\Gamma_\downarrow\epsilon-\Gamma_\uparrow\epsilon_e}{4}\cos\beta, \tag{A10}$$

with $\frac{d}{dt}n$ remaining the same as in Eq. (13).

APPENDIX B: CORRELATION FUNCTIONS AND THE REGRESSION THEOREM

Consider a unitary time evolution $U(\tau,t)$ where t is an initial time, at which the total density matrix is assumed to be factorized $\rho_E(t)\otimes\rho_S(t)$, into the environment ($E$) and system ($S$) density matrices, respectively. This is in line with the derivation of a Lindblad-type equations where the onset of system-environment entanglement is at time $t = 0$. Consider the correlation of two system operators $B(t+\tau)$, $A(t)$ (where the system has N states):

$$C(\tau,t) = \langle B(t+\tau)A(t)\rangle = \mathrm{Tr}_{E,S}\{U^\dagger(\tau,t)B(t)U(\tau,t)A(t)\rho_E(t)\rho_S(t)\}. \tag{B1}$$

We define $b(t) = A(t)\rho_E(t)\rho_S(t)$. Each element of the $N\times N$ matrix $U(\tau,t)b(t)U^\dagger(\tau,t)$ (with implicit environment indices) is a linear combination of all other elements. Hence, we can define a superoperator $K_{ij,lm}(\tau,t)$ that is an $N^2\times N^2$ matrix with system "superindices," such that

$$[U(\tau,t)b(t)U^\dagger(\tau,t)]_{ij} = \sum_{lm}K_{ij,lm}(\tau,t)b_{lm}(t). \tag{B2}$$

Since $A(t)$, $B(t)$, $\rho_S(t)$ are independent of environment indices we can trace over the environment and define a reduced time evolution for the system

$$K^{\mathrm{sys}}(\tau,t) = \mathrm{Tr}_E\{K(\tau,t)\rho_E(t)\}. \tag{B3}$$

Taking now $b(t) = \rho_E(t)\otimes\rho_S(t)$ in Eq. (B2) and tracing over ρ_E shows that $K^{\mathrm{sys}}(\tau,t)$ determines the time evolution of the system reduced density matrix $\rho_S(t+\tau) = K^{\mathrm{sys}}(\tau,t)\rho_S(t)$. The correlation becomes

$$C(\tau,t) = \mathrm{Tr}_S\left\{B(t)K^{\mathrm{sys}}(\tau,t)A(t)\rho_S(t)\right\} \tag{B4}$$

known as the quantum regression theorem [30].

In particular, for two-level open quantum systems with $N = 2$ we have the formal form $K^{\mathrm{sys}}(\tau) = e^{\hat{R}\tau}$, with $\hat{R}$ being a 4×4 matrix determined by the master equation, e.g., Eqs. (13) and (14). We calculate correlations of the form $C_{-+}(\tau) = \langle\sigma_-(\tau)\sigma_+(0)\rangle$ for $\tau > 0$ and $C_{-+}(-\tau) = C_{-+}^*(\tau)$ for $-\tau < 0$, hence, the Fourier transform

$$C_{-+}(\nu) = -2\,\mathrm{Re}\left\{\mathrm{Tr}\left\{\sigma_-\frac{1}{i\nu+\hat{R}}\sigma_+\rho_\infty\right\}\right\}, \tag{B5}$$

where $\rho_S(t)\to\rho_\infty$ is usually taken as the steady-state density matrix in a 4-vector form [43]. We note that since equilibrium is achieved on a finite timescale $\sim1/\Gamma$, on the long timescales of the Fourier transform one can choose instead another initial ρ, as long as it is not orthogonal to the steady-state one.

[1] C. W. Gardiner and H. Haken, *Quantum Noise*, Vol. 2 (Springer, Berlin, 1991).

[2] O. Hirota, A. S. Holevo, and C. M. Caves, *Quantum Communication, Computing, and Measurement* (Springer, New York, 2012).

[3] G. Lindblad, Commun. Math. Phys. **48**, 119 (1976).

[4] V. Gorini, A. Kossakowski, and E. Sudarshan, J. Math. Phys. **17**, 821 (1975).

[5] H. Breuer, P. Breuer, F. Petruccione, and S. Petruccione, *The Theory of Open Quantum Systems* (Oxford University Press, Oxford, 2002).

[6] T. H. Stievater, X. Li, D. G. Steel, D. Gammon, D. S. Katzer, D. Park, C. Piermarocchi, and L. J. Sham, Phys. Rev. Lett. **87**, 133603 (2001).

[7] C. Liu, Z. Dutton, C. H. Behroozi, and V. H. Lene, Nature (London) **409**, 490 (2001).

[8] A. N. Omelyanchouk, S. N. Shevchenko, Y. S. Greenberg, O. Astafiev, and E. Ilichev, Low Temp. Phys. **36**, 893 (2010).

[9] D. Farfurnik, A. Jarmola, L. M. Pham, Z. H. Wang, V. V. Dobrovitski, R. L. Walsworth, D. Budker, and N. Bar-Gill, Phys. Rev. B **92**, 060301(R) (2015).

[10] E. Togan, Y. Chu, A. S. Trifonov, L. Jiang, J. Maze, L. Childress, M. V. G. Dutt, A. S. Sørensen, P. R. Hemmer, A. S. Zibrov, and M. D. Lukin, Nature (London) **466**, 730 (2010).

[11] E. Geva, R. Kosloff, and J. L. Skinner, J. Chem. Phys. **102**, 8541 (1995).

[12] A. Muller, E. B. Flagg, P. Bianucci, X. Y. Wang, D. G. Deppe, W. Ma, J. Zhang, G. J. Salamo, M. Xiao, and C. K. Shih, Phys. Rev. Lett. **99**, 187402 (2007).

[13] E. B. Flagg, A. Muller, J. W. Robertson, S. Founta, D. G. Deppe, M. Xiao, W. Ma, G. J. Salamo, and C. K. Shih, Nat. Phys. **5**, 203 (2009).

[14] S. M. Ulrich, S. Ates, S. Reitzenstein, A. Löffler, A. Forchel, and P. Michler, Phys. Rev. Lett. **106**, 247402 (2011).

[15] A. Ulhaq, S. Weiler, S. M. Ulrich, R. Roßbach, M. Jetter, and P. Michler, Nat. Photonics **6**, 238 (2012).

[16] S. Baumann, W. Paul, T. Choi, C. P. Lutz, A. Ardavan, and A. J. Heinrich, Science **350**, 417 (2015).
[17] K. Yang, Y. Bae, W. Paul, F. D. Natterer, P. Willke, J. L. Lado, A. Ferrón, T. Choi, J. Fernández-Rossier, A. J. Heinrich, and C. P. Lutz, Phys. Rev. Lett. **119**, 227206 (2017).
[18] P. Willke, W. Paul, F. D. Natterer, K. Yang, Y. Bae, T. Choi, J. Fernández-Rossier, A. J. Heinrich, and C. P. Lutz, Sci. Adv. **4**, eaaq1543 (2018).
[19] G. Shavit, B. Horovitz, and M. Goldstein, Phys. Rev. B **99**, 195433 (2019).
[20] W. E. Lamb, Phys. Rev. **134**, A1429 (1964).
[21] B. Mollow and M. Miller, Ann. Phys. **52**, 464 (1969).
[22] R. E. Slusher and H. M. Gibbs, Phys. Rev. A **5**, 1634 (1972).
[23] R. Dum, A. S. Parkins, P. Zoller, and C. W. Gardiner, Phys. Rev. A **46**, 4382 (1992).
[24] F. Bloch, Phys. Rev. **70**, 460 (1946).
[25] J. Hauss, A. Fedorov, S. Andre, V. Brosco, C. Hutter, R. Kothari, S. Yeshwanth, A. Shnirman, and G. Schon, New J. Phys. **10**, 095018 (2008).
[26] A. Wallraff, D. I. Schuster, A. Blais, L. Frunzio, R.-S. Huang, J. Majer, S. Kumar, S. M. Girvin, and R. J. Schoelkopf, Nature (London) **431**, 162 (2004).
[27] J. Johansson, S. Saito, T. Meno, H. Nakano, M. Ueda, K. Semba, and H. Takayanagi, Phys. Rev. Lett. **96**, 127006 (2006).
[28] R. J. Glauber, Phys. Rev. **130**, 2529 (1963).
[29] B. R. Mollow, Phys. Rev. **188**, 1969 (1969).
[30] M. Lax, Phys. Rev. **129**, 2342 (1963).
[31] A. Ulhaq, S. Weiler, C. Roy, S. M. Ulrich, M. Jetter, S. Hughes, and P. Michler, Opt. Express **21**, 4382 (2013).
[32] C. Roy and S. Hughes, Phys. Rev. Lett. **106**, 247403 (2011).
[33] H. Kim, T. C. Shen, K. Roy-Choudhury, G. S. Solomon, and E. Waks, Phys. Rev. Lett. **113**, 027403 (2014).
[34] A. Redfield, in *Advances in Magnetic Resonance*, Advances in Magnetic and Optical Resonance, Vol. 1, edited by J. S. Waugh (Academic, New York, 1965), pp. 1–32.
[35] Y. C. Cheng and R. J. Silbey, J. Phys. Chem. B **109**, 21399 (2005).
[36] A. Suarez, R. Silbey, and I. Oppenheim, J. Chem. Phys. **97**, 5101 (1992).
[37] A. Levy and R. Kosloff, Europhys. Lett. **107**, 20004 (2014).
[38] P. Gaspard and M. Nagaoka, J. Chem. Phys. **111**, 5668 (1999).
[39] G. Kurizki, P. Bertet, Y. Kubo, K. Mølmer, D. Petrosyan, P. Rabl, and J. Schmiedmayer, Proc. Natl. Acad. Sci. USA **112**, 3866 (2015).
[40] E. Togan, Y. Chu, A. S. Trifonov, L. Jiang, J. Maze, L. Childress, M. V. Dutt, A. S. Sorensen, P. Hemmer, A. S. Zibrov, and M. Lukin, in *Frontiers in Optics 2011/Laser Science XXVII* (Optical Society of America, Washington, DC, 2011).
[41] J. Morton and B. Lovett, Annu. Rev. Condens. Matter Phys. **2**, 189 (2011).
[42] Z. L. Xiang, S. Ashhab, J. Q. You, and F. Nori, Rev. Mod. Phys. **85**, 623 (2013).
[43] I. Martin, A. Shnirman, L. Tian, and P. Zoller, Phys. Rev. B **69**, 125339 (2004).